BRANCH OFFICE

194 NASSAU STREET
PRINCETON, NEW JERSEY 08540
PHONE 924-4228

CR 73128

SYSTEMS TECHNOLOGY, INC.

13766 SOUTH HAWTHORNE BOULEVARD • HAWTHORNE, CALIFORNIA 90250 • PHONE 772-4421

Paper No. 55

A NEUROMUSCULAR ACTUATION SYSTEM MODEL

D. T. McRuer, R. E. Magdaleno, and G. P. Moore

USC–NASA CONFERENCE ON MANUAL CONTROL

March 1 – 3, 1967

University of Southern California
Los Angeles, California

CR 73128

A NEUROMUSCULAR ACTUATION SYSTEM MODEL*

D. T. McRuer, R. E. Magdaleno, and G. P. Moore
Systems Technology, Inc.
Hawthorne, California

Summary: Recently both high quality physiological data and human operator describing function data of low variability and large dynamic range have become available. These data lead to control engineering descriptions for neuromuscular actuation systems which are compatible with the available data and which provide insight into the overall human control structure (e.g., the types of feedback systems used for various inputs). In this paper, some of these physiological and human operator data are briefly reviewed, and a simple neuromuscular actuation system model is presented.

The physiological data of interest include recent anatomical and physiological data for the muscle spindle and input-output studies of the muscle. These data indicate that simple linear models can describe the basic behavior of these two elements in tracking tasks. Developed further here is the variation in system parameters as a function of average muscle tension, and the role of the muscle spindle both as an equalization element and in its effects on muscle tone.

The pertinent human operator describing function data include the covariation of high and low frequency phase data and the describing function variation of high frequency phase with tension.

The simplest neuromuscular model suggested by and compatible with these data is one in which muscle spindles provide both a feedback function, an operating point or bias adjustment, and at least one command path.

A. INTRODUCTION

The neuromuscular system is a composite of neural and muscular components situated in the spinal cord and the periphery — typically a limb and its neural connections — operating on commands sent from higher centers. We are interested in engineering descriptions of such systems in three respects:

Manual Control Engineering — The basic dynamics of the human operator and the precision of manual control are critically limited by the properties of the neuromuscular system. An

*This paper includes research efforts supported by the Ames Research Center, NASA, Moffett Field, California, under Contract NAS2-2824 and, under Contract AF 33(657)-10835, by the Air Force Flight Dynamics Laboratory (FDCC), Research and Technology Division, Wright-Patterson Air Force Base, Ohio.

understanding of this system has important practical ramifications in determining the effects of control system nonlinearities and sensitivities on manual control.

Control Theoretic — the neuromuscular system is an archetypical adaptive actuation system which, if understood operationally, might serve as the inspiration for analogous inanimate systems with similarly useful properties.

Physiological System Description — the study of the neuromuscular system as a biological servomechanism provides a framework for the interpretation and elaboration of neurophysiological data.

In what follows we first summarize some experimental data which have motivated our present model of the neuromuscular system. Then the components of the neuromuscular system are described, and simplified mathematical models for them are developed. These components are connected into a system structure and its operations for typical control situations are explored. Finally, the ability of the model to account for the experimental data is discussed.

B. HUMAN OPERATOR DATA INDICATING NEUROMUSCULAR SYSTEM EFFECTS

There is a large body of describing function data available for the overall human operator, (e.g., Refs. 1, 2, 3, and 4) as well as for the neuromuscular system, e.g., Refs. 5, 6, 7. In this paper we are interested in data that relate the effects of average muscle tension or tone on the neuromuscular system describing function data. These effects occur at very high and very low frequencies, so with measurements limited to mid-frequencies they show up primarily in the phase data.

1. High and Low Frequency Phase Covariation

To describe some recent operator dynamics data, several levels of approximation have been used (Refs. 3, 4, and 7). Two of these are shown in Fig. 1. These "describing function models" are descriptive of the transfer dynamics for the complete human operator including manipulator characteristics.* The so-called Precision Model is a minimum form compatible

*The describing function is written in terms of the frequency operator, $j\omega$, to emphasize that this kind of describing function is valid only in the frequency domain and exists only under essentially stationary conditions. For instance, it does not describe the system response to a discrete input, e.g., a step input (although some of the terms in the model may be compatible with portions of the step response time history).

Precision Model

Equalization and Gain | Basic Delays | Neuromuscular System

$$Y_p = K_p \left(\frac{T_L j\omega + 1}{T_I j\omega + 1}\right) e^{-j\omega\tau} \cdot \left\{ \underbrace{\left(\frac{\pm T_K j\omega + 1}{T_K' j\omega + 1}\right)}_{e^{-j\alpha/\omega}} \underbrace{\frac{1}{(T_{N_1} j\omega + 1)\left[\left(\frac{j\omega}{\omega_N}\right)^2 + \frac{2\zeta_N j\omega}{\omega_N} + 1\right]}}_{(T_N j\omega + 1)^{-1} \text{ or } e^{-j\omega T_N}} \right\}$$

where

$$\alpha \doteq \frac{1}{T_K'} \pm \frac{1}{T_K}$$

where

$$T_N \doteq T_{N_1} + \frac{2\zeta_N}{\omega_N}$$

Approximate Model

$$Y_p = K_p \left(\frac{T_L j\omega + 1}{T_I j\omega + 1}\right) e^{-j\omega\tau} \quad \frac{e^{-j\alpha/\omega}}{T_N j\omega + 1}$$

$$\doteq K_p \left(\frac{T_L j\omega + 1}{T_I j\omega + 1}\right) e^{-j[\omega(\tau + T_N) + (\alpha/\omega)]} \quad ; \quad \tau_e = \tau + T_N$$

FIGURE I. DESCRIBING FUNCTION MODELS

with all the fine detail, low variability data for random-appearing forcing functions and also compatible with such things as the dynamics of the movement component in step responses. The "Approximate Model" is a much simpler form in which the number of parameters is reduced without too serious a degradation in the analytical description of the data. Both models exhibit the same gain, equalization, and basic delay elements. They differ in their neuromuscular system aspects. For these the high frequency terms are third-order in the Precision Model. In the Approximate Model, the lower frequency effects of these third-order terms are approximated by either a first-order lag (so-called neuromuscular lag) or a pure time delay. The latter can be summed with the basic latencies to give an overall time delay, τ_e.

The very low frequency characteristics appear in the data primarily as a phase lag. In the Precision Model these characteristics are represented by the lead/lag, $(T_K j\omega + 1)/(T'_K j\omega + 1)$, which is a minimum form suitable to characterize both amplitude ratio and phase data completely for the limited data of extremely high precision [i.e., those data for controlled element forms K_c, K_c/s, and $K_c/(s - 1/T)$]. For many systems these low frequency effects can be further approximated, as derived below, by the single-parameter form $e^{-j\alpha/\omega}$. If the low frequency effects are modeled by transfer characteristics containing m lags and leads, then the incremental phase shift due to these will be

$$\Delta\varphi_{low} = \sum_{i=1}^{m} \tan^{-1}\left(\omega T_{lead_i}\right) - \sum_{i=1}^{m} \tan^{-1}\left(\omega T_{lag_i}\right)$$

At frequencies well above the break frequencies of these lags and lead, i.e., $\omega > 1/T_{lead_i}, 1/T_{lag_i}$, this can be approximated by

$$\Delta\varphi_{low} \doteq \sum_{i=1}^{m} \left(\frac{\pi}{2} - \frac{i}{\omega T_{lead}}\right)_i - \sum_{i=1}^{m} \left(\frac{\pi}{2} - \frac{1}{\omega T_{lag}}\right)_i$$

$$\doteq -\frac{1}{\omega} \underbrace{\sum_{i=1}^{m} \left(\frac{1}{T_{lead}} - \frac{1}{T_{lag}}\right)_i}_{\alpha}$$

We will use this $e^{-j\alpha/\omega}$ phase characteristic to approximate the mid-frequency effects of very low frequency leads and lags.

Our emphasis here will be on the α and equivalent time delay quantities contained in the Approximate Models exponential phase descriptor term, $e^{-j(\omega\tau_e + \alpha/\omega)}$. Figure 2 illustrates the nature of typical pilot describing function data and the application of the previously given Precision and Approximate Model forms as descriptors of these data. The typical data

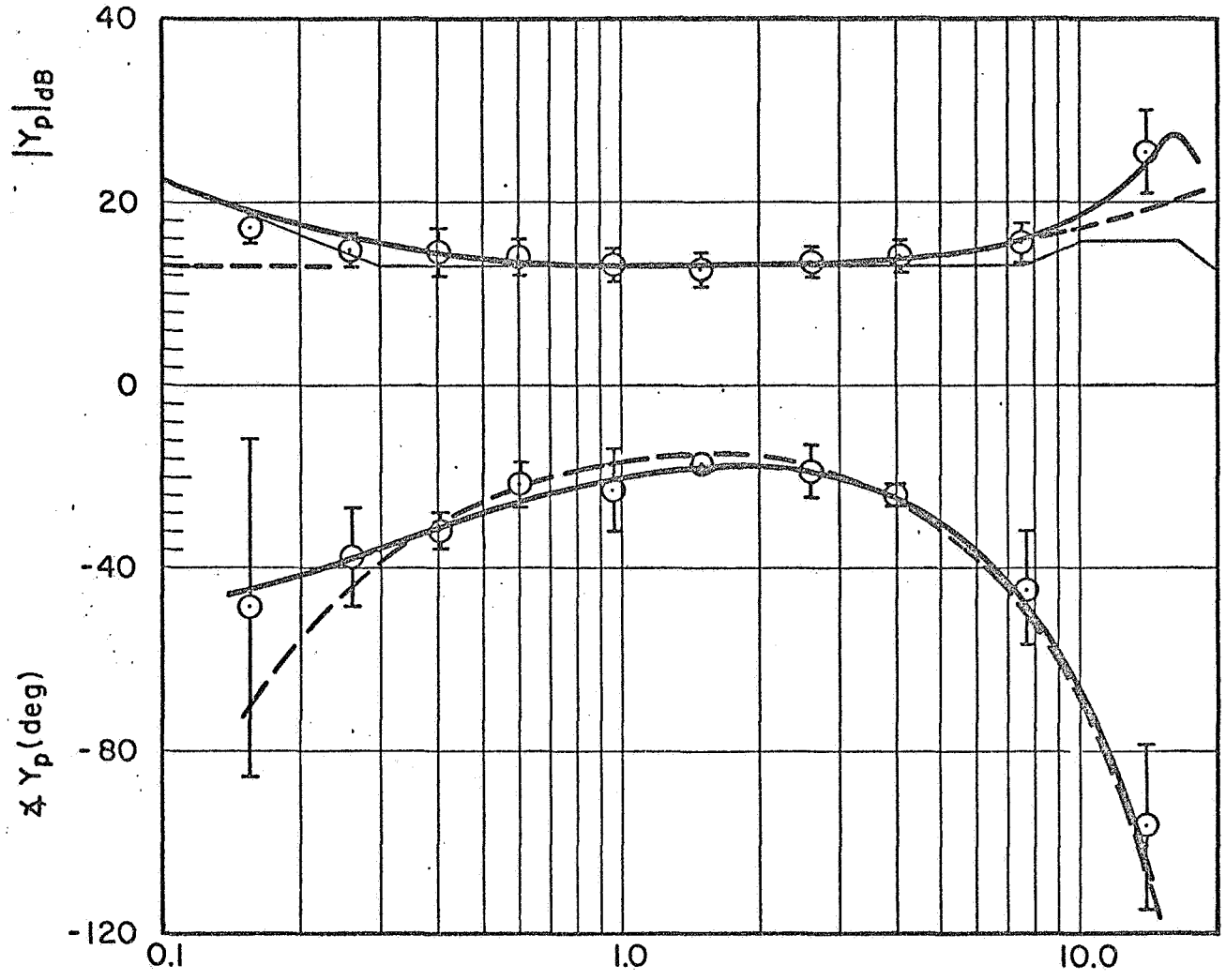

Precision Model (———)

$$Y_p = (25.1)\left(\frac{j\omega}{7.8}+1\right)e^{-0.09\,j\omega}\left\{\left(\frac{\frac{j\omega}{0.3}+1}{\frac{j\omega}{0.05}+1}\right)\frac{1}{\left(\frac{j\omega}{10}+1\right)\left[\left(\frac{j\omega}{16.5}\right)^2+\frac{2(0.12)}{16.5}\,j\omega+1\right]}\right\}$$

Approximate Model (— — —)

$$Y_p = (4.2)\left(\frac{j\omega}{7.8}+1\right)e^{-j[0.21\,\omega+(0.19/\omega)]}$$

FIGURE 2. TYPICAL PILOT DESCRIBING FUNCTION DATA AND MODELS

($Y_c = K_c/(s-2)$; $\omega_i = 4.0$ rad/sec)

(Ref. 2)

shown are from a so-called subcritical task involving the control of a controlled element, Y_c, consisting of a first-order divergence. The α and τ_e aspects do not affect the amplitude ratio at all, although they are clearly shown in the phase. The $\omega\tau_e$ phase due to time delay dominates the high frequencies, whereas the α/ω phase lag is the major low frequency effect. Their joint action tends to make the phase look like an umbrella, with α controlling the left side and τ_e the right side, i.e., changes in τ_e shift the right side of the umbrella, while changes in α shift the left. Simultaneous increases in both α and $1/\tau_e$ shift the umbrella to the right, whereas decreases shift it to the left.

Some idea of the variation of α and τ_e and their connections is provided in Ref. 7. Figure 3, which is taken from Ref. 7, indicates that α and $1/\tau_e$ vary together for the experiments considered there. In terms of the describing function phase curve shown in Fig. 2, both ends of the umbrella are shifted together in an adaptive response to forcing function bandwidth, ω_i, changes [for $Y_c = K_c/(s)^2$] or controlled element divergent time constant, T, changes [for $Y_c = K_c/s(s-1/T)$].

2. High Frequency Phase Variation With Tension

The effect of average voluntary muscle tension on the supination-pronation response to mechanical impulse inputs has been investigated in Ref. 5. The relative amount of muscle tension was inferred from a sphygmomanometer cuff attached around the forearm. This was displayed to the subject who then could readily set the reading to any one of five levels. These experiments were carried out using irregularly spaced mechanical impulses delivered, without warning, by a pendulum. The manipulator restraint consisted of an inertia several times larger than that of the arm, and the subject was asked to resist the perturbing influence of the pendulum-produced disturbance on the load.

The transient response resembled that of a dominant second-order system with light damping. Figure 4, taken from Ref. 5, shows the upper pole position of a complex pair fitted to the transient response for the five tension values (apparently for only one subject). In general, increasing mean tension increases the natural frequency of these roots but leaves the damping ratio relatively unchanged. We are interested in the effect of this trend on the high frequency phase which can be found by noting that, as in Fig. 1,

$$\frac{1}{1 + \left(\frac{2\zeta_N}{\omega_N}\right)j\omega + \left(\frac{j\omega}{\omega_N}\right)^2} \doteq \frac{1}{1 + \left(\frac{2\zeta_N}{\omega_N}\right)j\omega}$$

for frequencies below ω_N. Since all of the ω_N's are at the extreme upper end of the measurement bandwidth (see Fig. 2), then the approximate phase of these complex roots behaves as a simple lag with an effective time constant given by $2\zeta_N/\omega_N$. In the Approximate Model this is lumped into the overall time delay, τ_e.

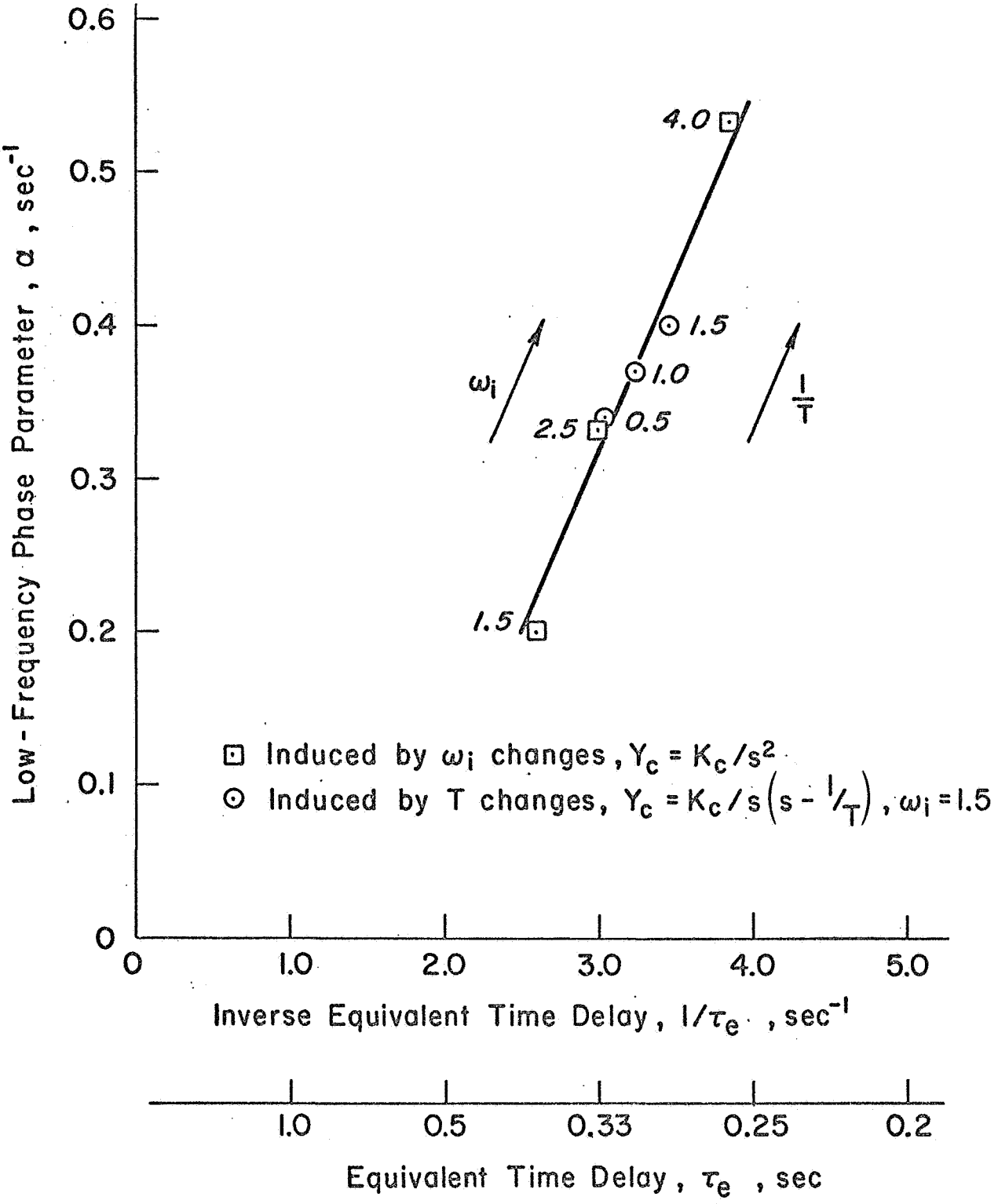

FIGURE 3. CONNECTION BETWEEN EQUIVALENT TIME DELAY AND LOW-FREQUENCY PHASE LAG

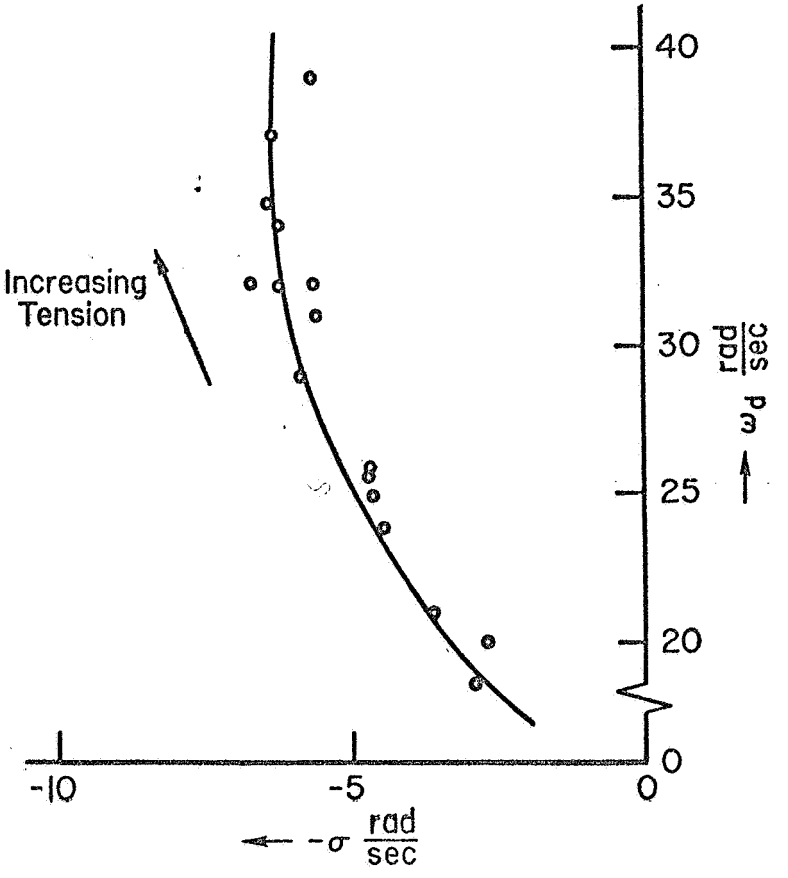

Figure 4. Root Locus of the Positive Pole of a Complex Pair Fitted to the Transient Response (Ref. 5)

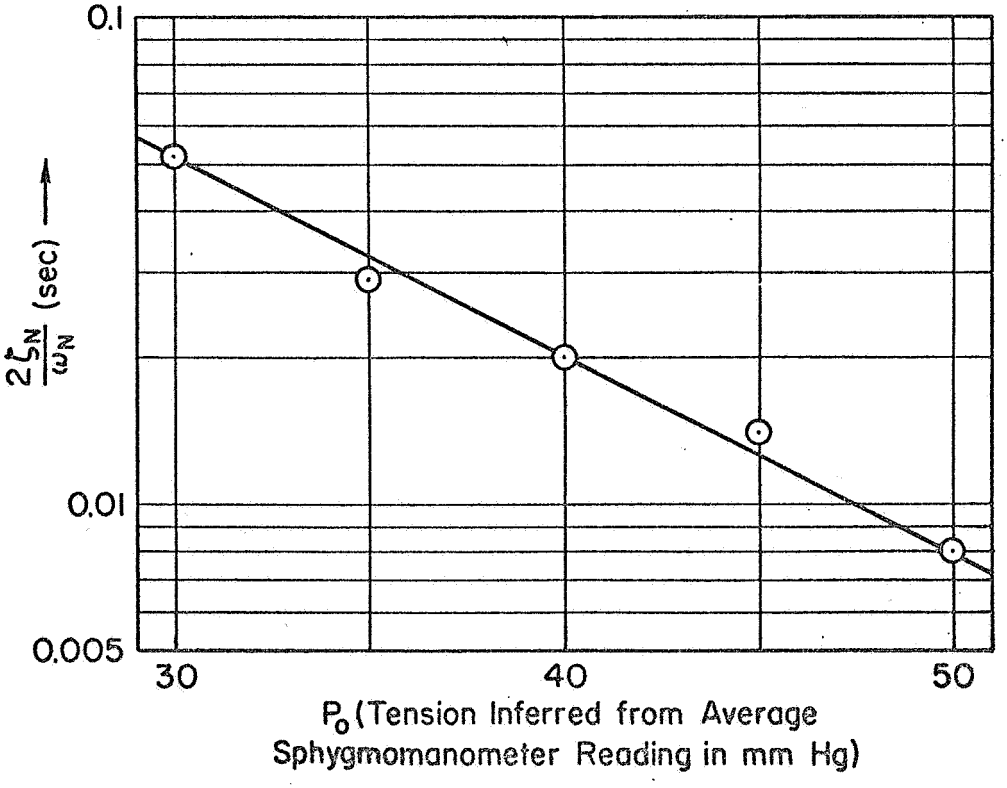

Figure 5. Effective Time Constant as a Function of Inferred Tension

Reference 5 also contained averaged data for three subjects which we can use to calculate the effective time constant for the five tension values (see Fig. 5). The decrease in time constant as tension increases will move the high frequency phase to the right.

C. DESCRIPTION OF THE COMPONENTS

1. Introduction

To describe the physiology of the neuromuscular system is very difficult because of the enormous complexities of the system and the many unknowns still present despite recent advances (Refs. 10, 11, and 12). In spite of these difficulties, we shall attempt here a broad and superficial coverage of some workings of the neuromuscular system elements, expressed in engineering terms. The components that shall be described are, in sequency: motor units; sensory units; interconnection and amplification elements. Only those elements which are believed to be important in the manipulation of spring-restrained low-inertia manipulators with negligible nonlinearities are considered.

2. Motor Units

The smallest functional entity in a motor system is a motor unit, which is illustrated schematically in Fig. 6. It consists of a motorneuron cell body, located in the ventral horn of the spinal cord; its axon,* which is a single-fiber signal-transmission line from the cell body to the muscle; and the group of muscle fibers connected to the terminal branches of the axon. Motor units differ primarily in the number of muscle fibers (innervation ratio) served by one motorneuron. The innervation ratio is a limiting factor in the attainable precision of muscle control. For muscles involved in very precise and finely graded movements, such as those of the eye, the innervation ratio can be as low as about five. In contrast, large muscles which are used primarily in gross movements, such as the biceps, may have hundreds or thousands of muscle fibers per motorneuron. The individual fibers of muscles are grouped into bundles which, in turn, are assembled to make up the complete muscle. There may be as many as several million fibers in a muscle. The fibers of a motor unit are widely dispersed in several bundles, so the action of a single motor unit is spread throughout the muscle.

The muscle responds to the commands carried by the motorneuron. These responses are transmitted along the axon as brief ($\sim$1 msec) electrical pulses of essentially invariant shape and duration, which travel at rates

---

*These axons to skeletal muscle fibers are the largest of the motor fibers and have diameters which are in the "alpha" range (12–20μ). Hence these motor neurons are sometimes called "alpha motorneurons."

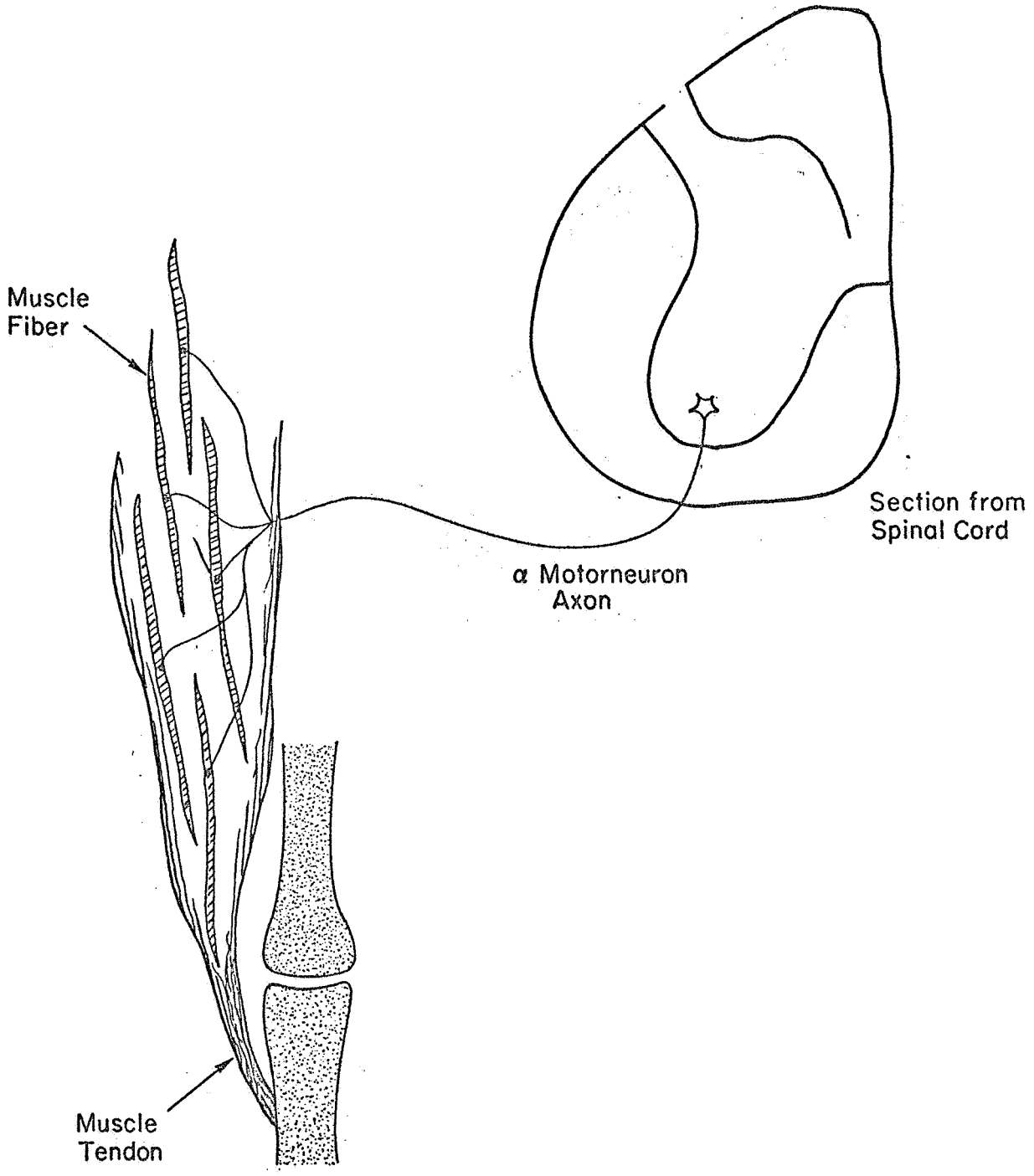

Figure 6. Diagram of a Motor Unit

of up to 100 m/sec. Arriving at the axon muscle interface ("neuromuscular junction") they trigger the release of a chemical agent which induces the generation of a similar pulse in the muscle fiber; the pulse spreads over the fiber, triggering a sequence of events leading ultimately to contraction of the muscle fiber.

The net result of all this activity is a brief contractile response of the muscle fiber, called a "twitch." A typical twitch time history for isometric conditions (limb constrained so that the muscle system is of essentially constant length) is shown in Fig. 7. This amounts to the impulse response of the muscle fiber portion of a motor unit. It is also the weakest possible natural movement involving that muscle. The twitch shown is typical of a fast muscle, with a contraction time of about 40 ms and a far longer decay.

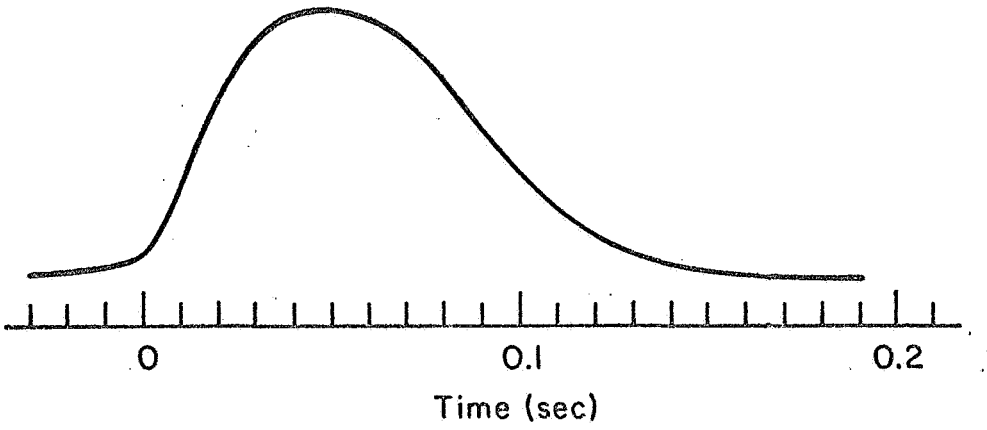

Figure 7. Impulse Response of a Muscle Fiber

In a single motor unit a low repetition rate of action potentials arriving at the motor endplate causes a train of essentially independent twitches. In each of these the mechanical response lasts far longer than the action potential stimulus. As the frequency of excitation increases, a second action potential will arrive while the mechanical effect of the prior stimulus still persists, causing a mechanical summation or fusion of contractions. Up to a point the degree of summation increases as the stimulus interval becomes shorter, although the summation effect decreases as the interval between the stimuli approaches the refractory period of the muscle. Maximum tension occurs when the excitation frequency is so high that the degree of summation approaches zero. This limiting response is called a tetanus, and the tension developed is bout four times that of a single twitch.

In an actual muscle system there are many motor units energized by many coordinated motorneurons. Thus, when more force is needed, not only can a single motor unit be fired more rapidly, but other motor units can be activated and their motorneurons made to discharge more frequently.

By this means, the degree of tension in a muscle is directly related to the number of active motorneurons and to the rate of spike discharge in these motorneurons. This provides for an enormous dynamic range in a given muscle.

Although deficient in detail, the above summary provides a broad qualitative picture of the major electrical and chemical events involved in the translation of a motorneuron command to a muscle response. The picture can be put into analytical form by treating existing data on muscles as if they were force/speed characteristics of an actuator. This can be done using actual data or, alternatively, by using equations fitted to actual data. The second scheme is by far the more convenient. The most popular data summary in equation form for muscles is Hill's equation. It has been found suitable for a wide range of muscle types, including arm muscles in man (Ref. 13). Hill's "characteristic equation" (Refs. 13 and 14) is

$$(F + a)V = b(P_T - F) \tag{4}$$

where F is the force exerted by the muscle during a contraction with a velocity, V, P_T is the isometric (V = 0) or maximum (tetanic) tension in the muscle, and a and b are constants. Note that P_T depends upon muscle length—this will be taken into account in a later paragraph. In this equation FV is the power required to do mechanical work and aV may be considered to be the power dissipated in heat within the muscle.

Hill's equation is often presented in terms of a force/velocity relationship,

$$(F + a)(V + b) = b(P_T + a) \tag{5}$$

In this connection a and b become so-called force and velocity constants. In terms of the modified force and velocity variables, i.e., (F + a) and (V + b), the relationship is hyperbolic (see Fig. 8), implying constant "power" in these coordinates for a constant isometric tension. Referring to Fig. 8, Hill's equation has been found to be most accurate for shortening conditions and to depart from the hyperbolic relationship for lengthening velocities. The relationship tends to be more linear and somewhat steeper than an extrapolation from Hill's equation would show. This results in a change in slope in the region of most interest (small positive and negative velocities). However, in the context of an agonist-antagonist muscle pair one muscle will be lengthening while the other is shortening. Thus, the overall force/velocity relationship will be continuous.

Also shown in Fig. 8 are curves (Ref. 16) for the force/velocity relationship for a number of different levels of average electrical activity measured from surface electrodes. These indicate that Hill's equation also applies if P_T is replaced by P, the isometric tension in the muscle due to the average firing rate, f, of the motor unit ensemble. Note also that the slope of the force/velocity curves increases for increasing average firing rate, i.e., the effective damping varies with muscle activity.

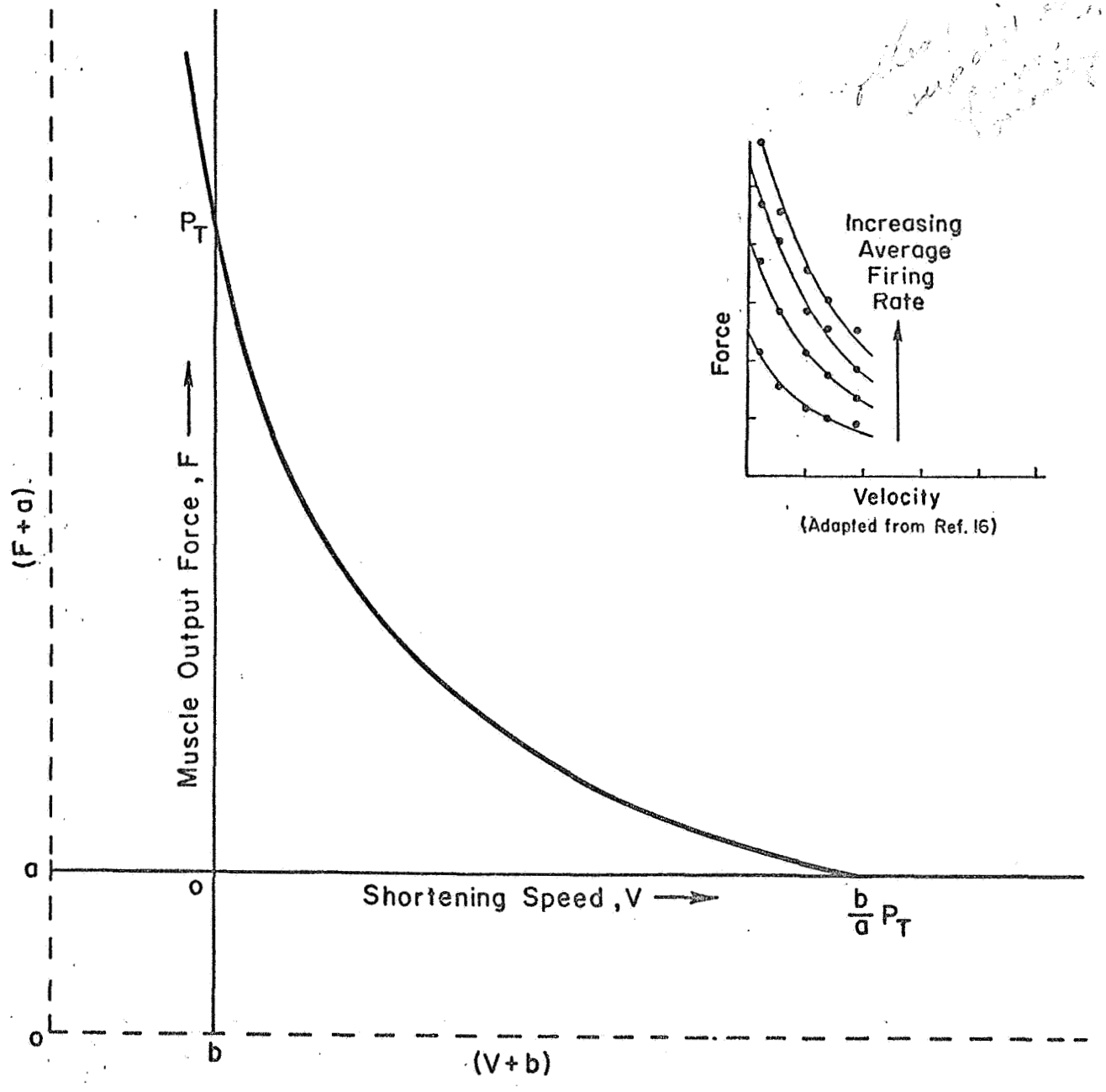

Figure 8. Force/Speed Relationship for Muscle, P_T = Constant

When written in the form desired for our purposes, Hill's equation will be

$$F = \frac{bP}{b + V} - \frac{aV}{b + V} \tag{6}$$

We shall be interested primarily in situations where the muscles involved execute small perturbations about the operating point $P = P_o$, $V_o = 0$. For these circumstances, the velocity, V, can be considered small and Eq. 6 can be expanded in a Taylor series. Assuming that terms of the second-order or higher in perturbation quantities are negligible yields

$$F = F(P_o + \Delta P, V_o + \Delta V) \doteq F(P_o, V_o) + \left[\frac{\partial F}{\partial P}\Delta P + \frac{\partial F}{\partial V}\Delta V\right]_{\substack{P = P_o \\ V = V_o = 0}} \tag{7}$$

Evaluating the partial derivatives and setting $\Delta V = V$ yields

$$F \doteq \underbrace{P_o + \Delta P}_{P} - \left(\frac{a + P_o}{b}\right)V \tag{8}$$

The general tension, P, in Eq. 8 is a function of both length and average firing rate as shown in Fig. 9. The zero and maximum lines on this figure are from Ref. 8, whereas the dashed lines for other average firing rates represent an interpretation of the data in Ref. 9. For a control task in which the muscle will have an average tension, P_o, average firing rate, f_o, and average or rest length, L_o, we can describe small deviations about the operating point with a Taylor series expanded about $f = f_o$ and $L = L_o$. Keeping only terms of first order in the perturbation quantities yields (for the tension, P, near P_o)

$$P = P(f_o + \Delta f, L - \Delta L) \doteq P_o(f_o, L_o) + \left[\frac{\partial P}{\partial f}\Delta f - \frac{\partial P}{\partial L}\Delta L\right]_{\substack{f = f_o \\ L = L_o}}$$

$$\doteq P_o + C_f\Delta f - \frac{\partial P}{\partial L}\Delta L \tag{9}$$

where ΔL has been defined as positive in the direction of muscle shortening so that $d(\Delta L)/dt$ will equal shortening velocity. Thus the muscle output force contains a steady component, a component sensitive to changes in firing frequency and an effective spring element. Substitution of Eq. 9 into Eq. 8 gives the result

$$F \doteq P_o + C_f\Delta f - \left(\frac{a + P_o}{b}\right) V - \frac{\partial P}{\partial L}\Delta L$$

$$\doteq P_o + C_f\Delta f - B_M V - K_M \Delta L \qquad (10)$$

In terms of an analogous physical system the linearized equation for a muscle given above corresponds to a force source, $P_o + C_f\Delta f$, coupled to a parallel spring-viscous-damper combination. Such a model is generally sufficient when the muscle is operating near or below the natural muscle length in the body. When the muscle is substantially greater in length, the elastic element may become negative. Except for this consideration, the equivalent elastic element has approximately constant gradient. The damper element, on the other hand, has a damping coefficient which is linearly related to the operating point tension. Consequently, the effective damping is also directly proportional to f_o, the steady-state firing rate, since $P_o = C_f f_o$.

Skeletal muscles can only contract actively, so movements involving high-grade skill, such as tracking, generally require coordinated groups of muscles. The simplest of these is an agonist/antagonist pair connected at opposite ends of a first-class lever to provide rotary motion. For rotation to occur one muscle must contract while the other extends. If the opposing muscles each have a steady-state tension in the static situation caused by some steady-state or average firing rate, f_o, rotation can be accomplished by increasing the firing rate for the contracting muscle by the increment Δf while simultaneously decreasing the firing rate in the antagonist by about the same increment.

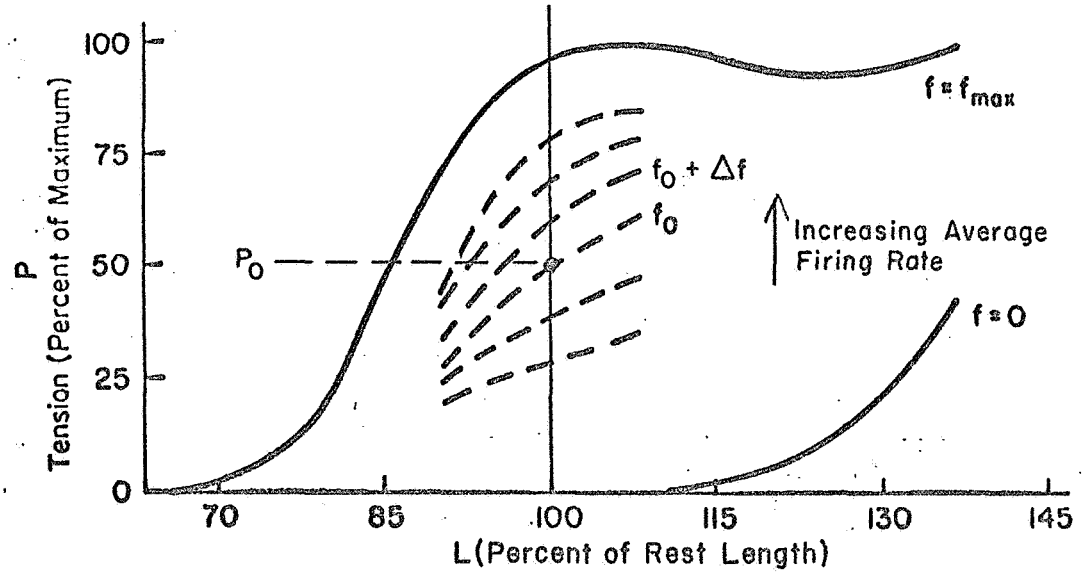

Figure 9. Presumed Tension-Length Curve (from Refs. 8 and 9)

The actual muscle system involved in almost any complex limb motions is seldom, if ever, as simple as that described above. However, the same principles hold for each agonist/antagonist pair involved and a grand summation can be made of all the pairs contributing to the actual limb motion of interest.

In tracking actions the muscle system operates in conjunction with a manipulator, which is ordinarily restrained by both linear and nonlinear mechanical elements. If linearity is assumed here, the load dynamics of a wide variety of practical manipulators can be characterized adequately by spring, damper, and inertia elements in parallel. Under these conditions the limb/manipulator load dynamics for the pilot's actuation system under perturbed conditions will appear as shown in Fig. 10.

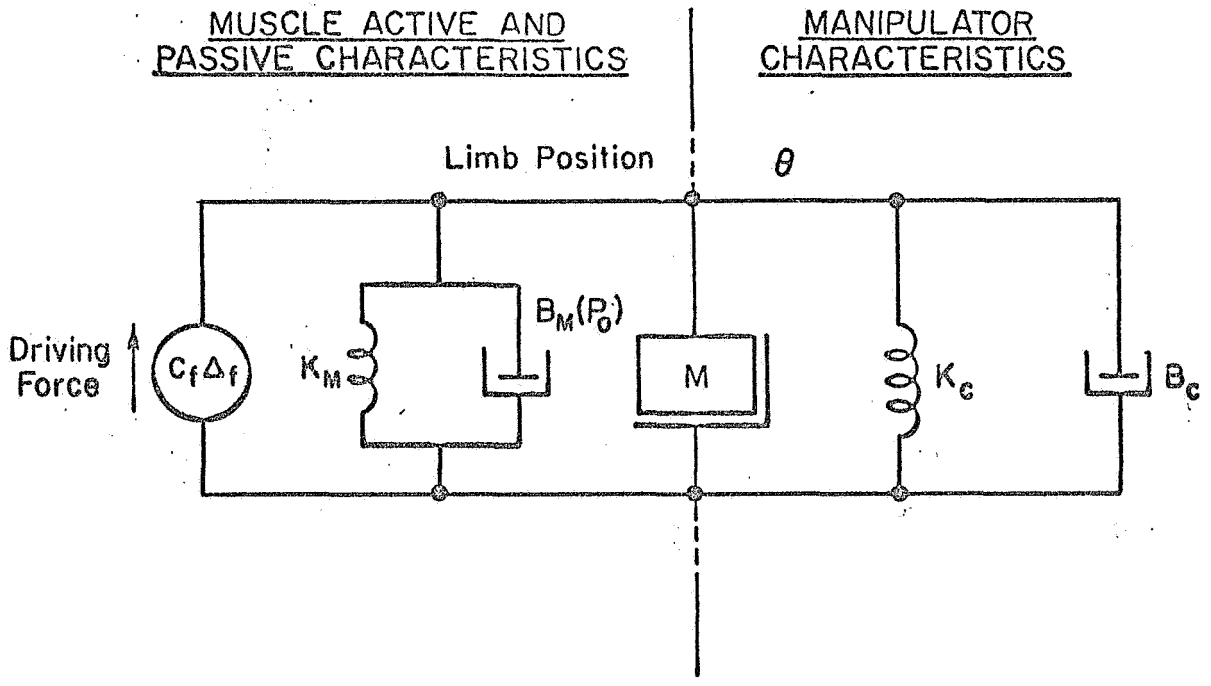

Figure 10. Schematic of Limb/Manipulator Load Dynamics for Pilot's Neuromuscular Actuation System

Since the limb inertia and the manipulator inertia are in parallel, the two are lumped together in the single effective inertia, M. The transfer function between limb rotation and differential firing rate will then be

$$\frac{\theta}{\Delta f} \doteq \frac{\frac{C_f}{M}}{s^2 + \left[\frac{B_M(P_o) + B_c}{M}\right] s + \frac{K_M + K_c}{M}} \qquad (11)$$

For a particular limb/manipulator system the undamped natural frequency

$$\omega_M = \frac{K_M + K_c}{M} \tag{12}$$

will be constant as long as the motions do not require muscle lengths which depart too far from L_o. The damping characteristics, on the other hand, will vary directly with the average tension, P_o, which is subject to enormous variation. Consequently, the damping ratio

$$\zeta_M = \frac{B_c + B_M(P_o)}{2\sqrt{(K_M + K_c)M}} \tag{13}$$

can vary greatly. With a normal subject the minimum average tension in movements having zero mean is $P_o = 0$, so the minimum limb/manipulator system damping ratio will be

$$\zeta_o = \frac{B_c}{2\sqrt{(K_M + K_c)M}} \tag{14}$$

For precision movements in tracking there is always some average tension acting, and ordinarily this is sufficient to make the damping ratio considerably greater than unity. For this case the appropriate forms for Eq. 11 are, therefore, either

$$\frac{\theta}{\Delta f} = \frac{\dfrac{C_f}{(K_M + K_c)}}{\left(\dfrac{s}{\omega_M}\right)^2 + \dfrac{2\zeta_M}{\omega_M} s + 1} \tag{15}$$

or, when $\zeta_M > 1$,

$$\frac{\theta}{\Delta f} = \frac{\dfrac{C_f}{(K_M + K_c)}}{\left(T_{M_1} s + 1\right)\left(T_{M_2} s + 1\right)} \tag{16}$$

The dynamics of this equivalent system are illustrated for two cases of tension by the $j\omega$-Bode diagram of Fig. 11. From this it is apparent that the effect of changing the viscous characteristic of the muscle group is to decrease the high frequency time constant, T_{M_2}, and increase the low frequency time constant, T_{M_1}. In the process the width of the −20 dB/decade

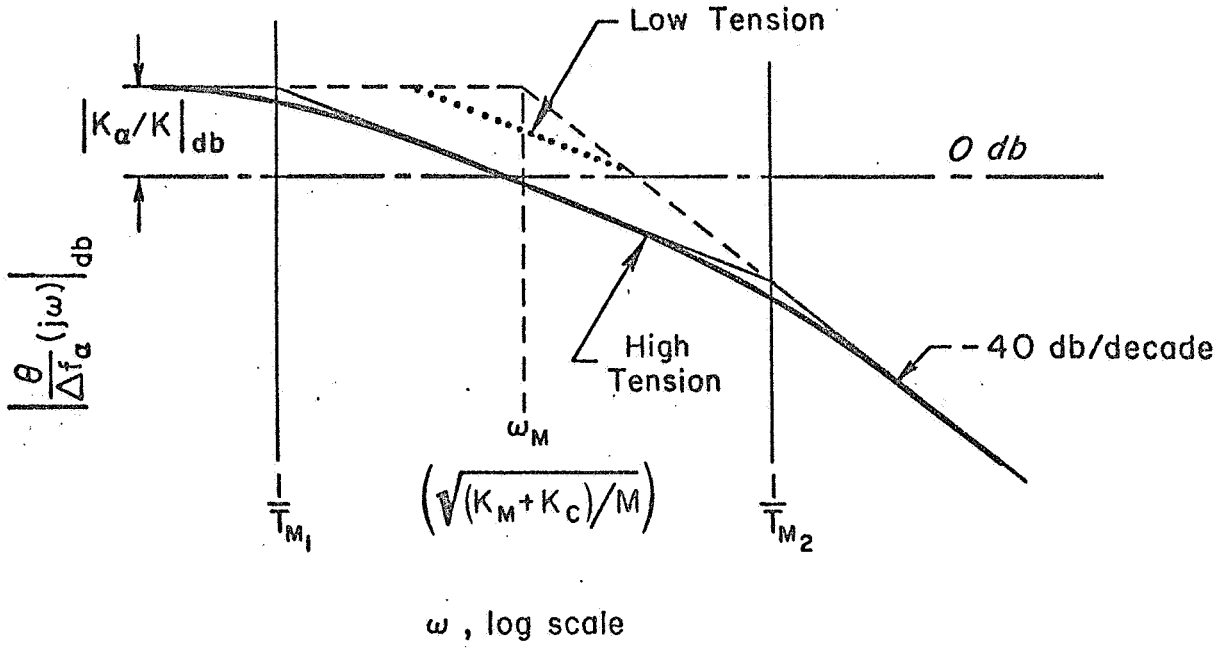

Figure 11. jω-Bode Diagrams for Limb/Manipulator Dynamics

portion on the limb/manipulator system Bode diagram is increased. As will be seen later these changes, due to an increase in steady-state tension, have most important consequencies on the neuromuscular system dynamics.

3. Muscle Spindles

a. Spindle Anatomy. Much of the control of neuromuscular behavior in the periphery is dependent on a complex organ located in most muscles of the body, the muscle spindle. It is in itself a complex neuromuscular integrative system receiving a continuous set of motor control and command signals from the central nervous system, and sending a constant stream of sensory information signals via its several paths back to the central nervous system.

A typical muscle may have 50–80 of these organs, embedded at various points among the tension-producing ("extrafusal") muscle fibers of the main muscle mass (Ref. 17). A typical spindle is elongated in shape, may be several millimeters in length, and has an orientation parallel to that of the extrafusal muscle fibers. They may be arranged in isolation, in tandem with each other, or be found in conjunction with other specialized receptor structures of the muscle.

Since the influence of the spindle in neuromuscular control is more far-reaching than previously suspected, it is important to review some of its basic anatomical and physiological features. These have been documented in several recent journals and symposia (Refs. 18–20) and

in what follows we shall present a summary of this work in which the complexities of spindle structure and function not relevant to the present discussion are either simplified or omitted.

A highly simplified diagramatic view of a muscle spindle is shown in Fig. 12. This shows the central axis of the spindle which consists of a globular nuclear bag region connected to either pole of the spindle by means of a pair of nuclear bag fibers, which are themselves typical striated muscle fibers (~25 μm in diameter).* These nuclear bag fibers are known as "intrafusal fibers," and are never observed to contribute directly to the development of tension in the muscle. Rather, they appear to be motor fibers related solely to control within the spindle itself. From their microscopic appearance the bag fibers appear to be normal striated muscle fibers and hence would be expected to have dynamic and mechanical properties similar to those of the extrafusal fibers discussed in the previous section.

The nerves supplying the intrafusal fibers have their cell bodies situated in the spinal cord and are connected to them by axons which have a diameter somewhat smaller than that of the axons connected to extrafusal muscle fibers. To distinguish these two classes of motor cells, axons and muscle fibers, the terms "gamma" (referring to the spindle motor system) and "alpha" (referring to the main muscle motor system) are used.

Of equal importance to these effector or command paths, however, are the sensory fibers which originate at the spindle and which generate pulse trains carrying information back to the spinal cord. In a typical spindle, there will usually arise one large axon whose principal termination winds around the nuclear bag region (a region of the spindle without muscle or contractile elements). These are the primary or annulospiral endings. The Type Ia axons serving these have large diameters (12–20 μm) and do not have terminations with other spindles. A second type of sensory ending is the flower-spray or secondary ending (not shown in Fig. 12). Each axon can terminate in several endings along the intrafusal fiber. These Type II axons are about half the diameter of the Type Ia afferents. They never appear to terminate in the nuclear region of the bag fiber, but the same Type II axon can have terminations in more than one spindle.

In the present paper we shall be concerned only with the behavior of the larger diameter primary endings — how they respond to changes in muscle length and gamma activity.

Before summarizing the physiological behavior of the primary ending, we must first indicate something about the relation between mechanical events at the nuclear bag region and the electrical events in the sensory

---

*Chain fibers, which lack the nuclear bag region, have been observed and discussed (Ref. 18). They have smaller diameters and are connected in series and in parallel with the nuclear bag fibers. All spindles have at least one nuclear bag fiber, but may not have any chain fibers. Thus we shall assume that the chain fibers are not vital to the spindle's basic behavior.

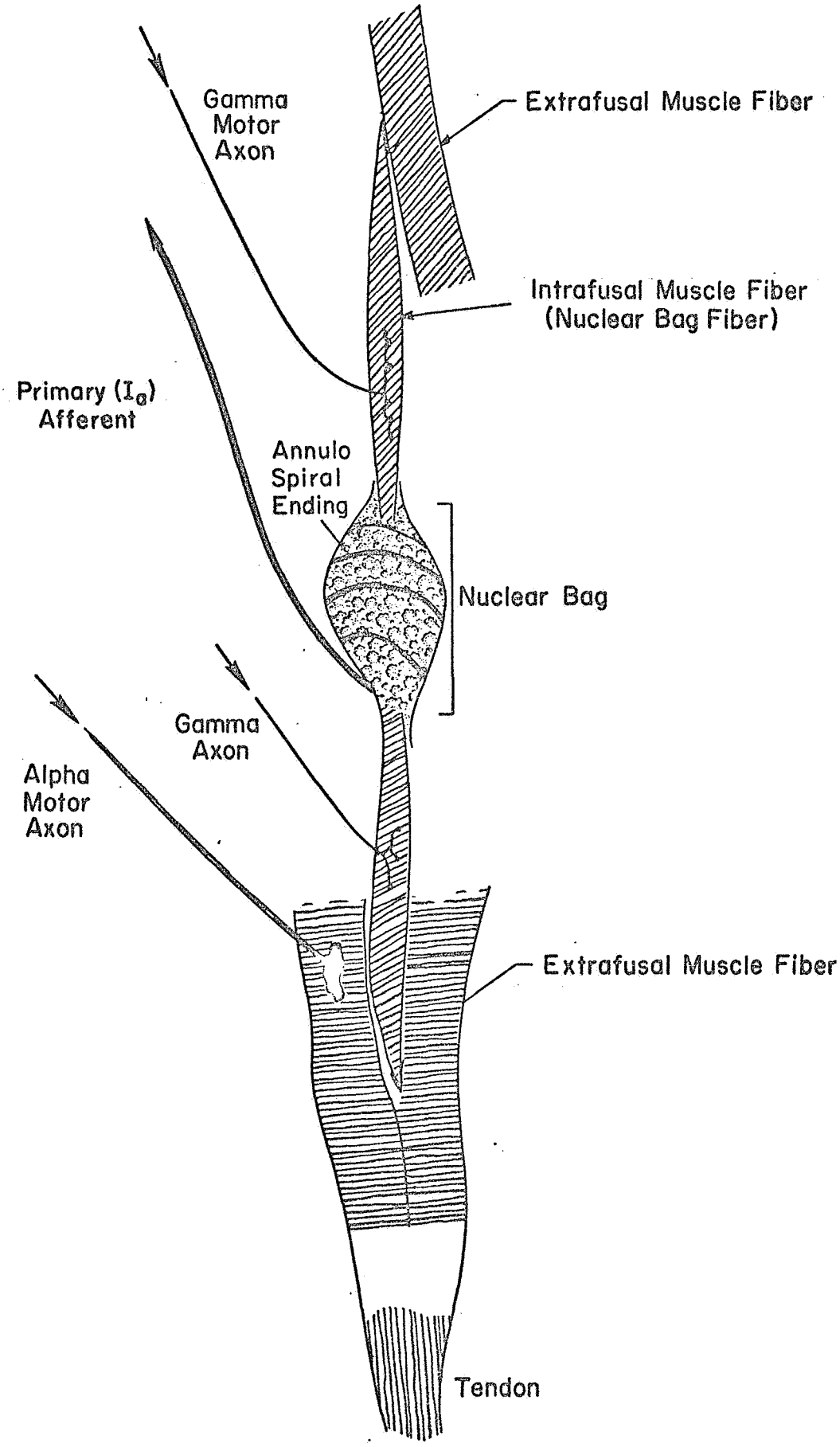

Figure 12. Idealized Nuclear Bag Muscle Spindle

annulospiral nerve ending. Much evidence has been accumulated which indicates that mechanical deformations of sensory terminals lead to the development of electrical potential fields at the terminals which are directly proportional to the strength of the deformation (Ref. 23). These generator potentials in fact are very accurate mappings of the forces operating on the terminals and can follow rather high frequencies of change in the deforming stimulus. The fields are an inherent property of the receptor membrane itself, and the fields are utilized by the sensory axon in the production of nerve impulses in specialized triggering regions near the receptor endings. Nerve impulses, in fact, are generated at a rate directly proportional to the magnitude of the generator potential, hence there is a continuous transmission of impulses at a frequency which is a linear function of that potential and hence of the strength of the deformation. The system exhibits a high degree of sensitivity to length changes; a significant shift in firing frequency can result from length changes of only a few microns (Ref. 24). We can use this relationship to reconstruct the time course of tension changes at the nuclear bag region from observed trains of nerve impulses.

b. Physiology of the Spindle Primary Ending. In this section we will briefly consider some of the data concerned with input/output relations in the primary (annulospiral) ending of the spindle. First we will consider the steady-state relations between the firing frequency in the spindle Ia axon as a function of muscle length, and how this is influenced by gamma activity. Next we will present data regarding the response of the primary ending to transient changes in muscle length and how such responses are modified by gamma activity. Finally, we shall consider the response of the primary ending to gamma stimulation alone.

On the basis of these data we will present a small-signal equivalent lumped-parameter mechanical model of the spindle whose parameters are under gamma control.

The primary ending of a spindle usually shows some spontaneous discharge even when the extrafusal muscle fibers are at their normal resting body length. This is presumably due to a small amount of residual tension in the spindle. Even in the absence of any motor signals from the cord, this spontaneous rate of firing in the spindle will increase monotonically as a function of increasing muscle length (from a few pulses per second to a hundred or more pulses per second). This arises because the disposition of the spindle within the muscle serves to transmit length changes in the muscle to the bag region where the change is reflected as an increase in bag tension. Conversely, shortening of the muscle (either passively or in response to an alpha motor command signal) will reduce the tension on the bag and hence reduce the spindle Ia sensory fiber firing frequency.

Figure 13 shows some typical plots of spindle sensory receptor firing frequency as a function of muscle length. Over a considerable range this relation is linear.

Recent studies of single gamma fibers ending on spindles whose primary endings were being monitored have shown that repetitive stimulation of certain gamma fibers will produce a response which consists of a general

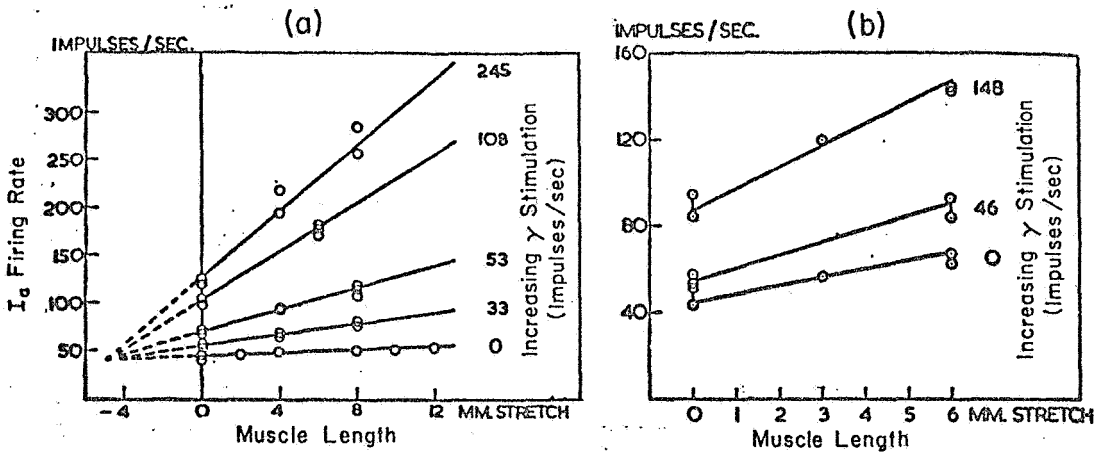

Figure 13. Steady-State Length — Ia Firing Rate Relations for Various Gamma Fiber Stimulation Rates (Reproduced from Ref. 26)

increase in the firing rate of the primary ending (relative to its control rate) as a function of muscle length. This may result in (1) a simple translation of the length-frequency curve upward (Fig. 13a), or (2) a family of curves of increasing slope whose relations are still essentially linear (Fig. 13b), or (3) in a combination of both (Refs. 25, 26). Each family of curves is a function of the stimulation frequency of the gamma fiber.

The shift in length-frequency relation is usually unaccompanied by any significant increase in the velocity sensitivity of the fiber (see below), i.e., the gamma fiber has influenced only the static gain of the primary ending; such a gamma fiber is designated as a static fusimotor fiber.

Thus, Fig. 13 shows that the discharge frequency of the primary fiber as a function of muscle length remains linear under static gamma stimulation. The base firing frequency at zero extension increases as gamma firing rate increases, hence the steady-state behavior can be described by an equivalent variable-slope spring element plus a bias level, both under static gamma control.

In addition to this static length-firing frequency relation, the primary ending also shows a strong velocity sensitivity to stretch or release in which its firing frequency, with rapid lengthening, can increase to several hundred pulses per second, regardless of length, and characteristically drops abruptly to zero for many seconds when the muscle is allowed to shorten.

This velocity-sensitive property can also be influenced by gamma stimulation, but the population of gamma fibers with this capacity is distinctly different from that which influences the static relation. Gamma fibers which increase the velocity-sensitive or dynamic part of the

response to changes in muscle length with only a small effect on the static gain are those called dynamic fusimotor fibers. The effect of stimulating these is also dependent on the stimulating frequency. Thus, the primary ending exhibits an inherent relation between firing rate, length, and velocity; the static gamma fiber increases its discharge for a given length (but in fact may decrease its relative sensitivity to stretch). Conversely, the dynamic fiber greatly increases the firing frequency of the primary ending during stretch, but leaves its initial and final frequencies essentially unchanged.

Our interpretation of the present knowledge of the behavior of the primary sensory ending can be summarized by the simplified mechanical network in Fig. 14. Here we shall confine our attention to the nuclear bag fiber. The intrafusal fibers are represented as typical skeletal muscle fibers, i.e., as an elastic element (K_F) in series with a parallel elastic-viscous unit (K_N and B_N). The nuclear bag region is represented as a simple elastic element (K_S).

Since the steady-state firing rate and the slope of the length-frequency curves are under static gamma control, a static gamma (γ_s) driven force generator and a variable K_F are indicated conjecturally in the diagram. Similarly, B_N and K_N are indicated as variable under dynamic gamma control, and are in parallel with a dynamic gamma (γ_d) driven force generator. K_S is assumed fixed. Referring to this figure, we see that a step change in muscle length or a step change in static gamma activity will change the primary ending firing rate as in a typical lead/lag network step response (Ref. 10). Step changes in dynamic gamma activity may produce some changes in sensory fiber firing rate, but these will show a smooth rise without overshoot. The principal effect, however, will be to markedly alter subsequent responses to static gamma stimulation or muscle length changes. The force generator, γ_s (shown dotted), can be replaced by the effective length input, γ_c, at least as far as the response at X_S (stretch of the nuclear bag ending spring, K_S) is concerned.

A step change in the effective-length input signal (via a step in γ_c or L) will initially be taken up across K_F and K_S, since the damper will not allow sudden position changes. Subsequently the length change across K_S and K_F will be redistributed between the three springs (K_F, K_N, and K_S), thus reducing the displacement across K_S. Thus the primary ending firing rate will respond in proportion to deformation of X_S, which will have the form

$$\Delta f_s = C_{f_s} X_S = \frac{K_{sp}(T_K s + 1)}{aT_K s + 1} (\gamma_c - L) + \frac{C_d \gamma_d}{aT_K s + 1} \qquad (17)$$

4. Central Closed-Loop Neuromuscular Reflex Connections

The sensory fibers leaving the muscle spindle enter the spinal cord and form direct synaptic connections with the motorneurons supplying the

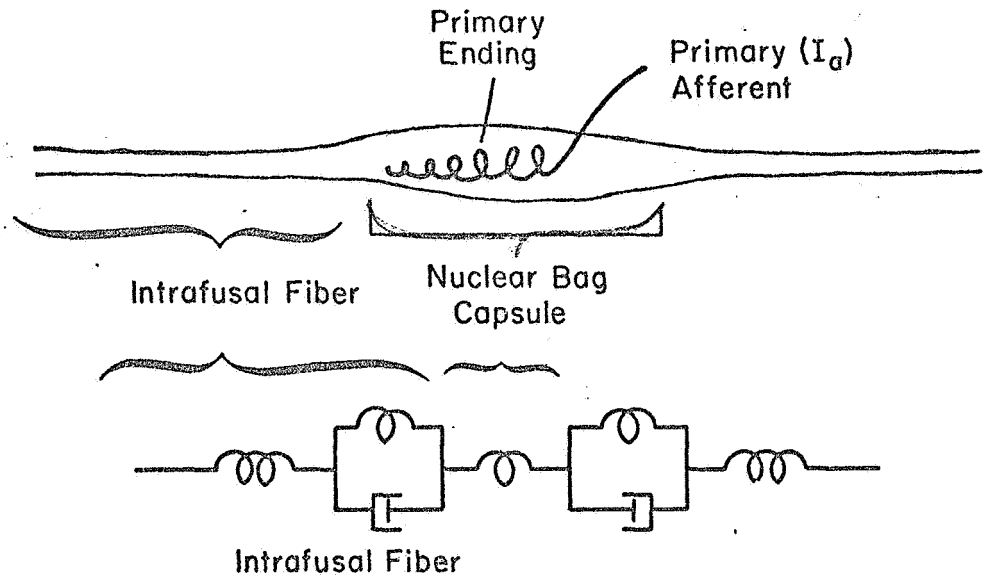

(a) Spindle and Equivalent Lumped Parameter Mechanical Network

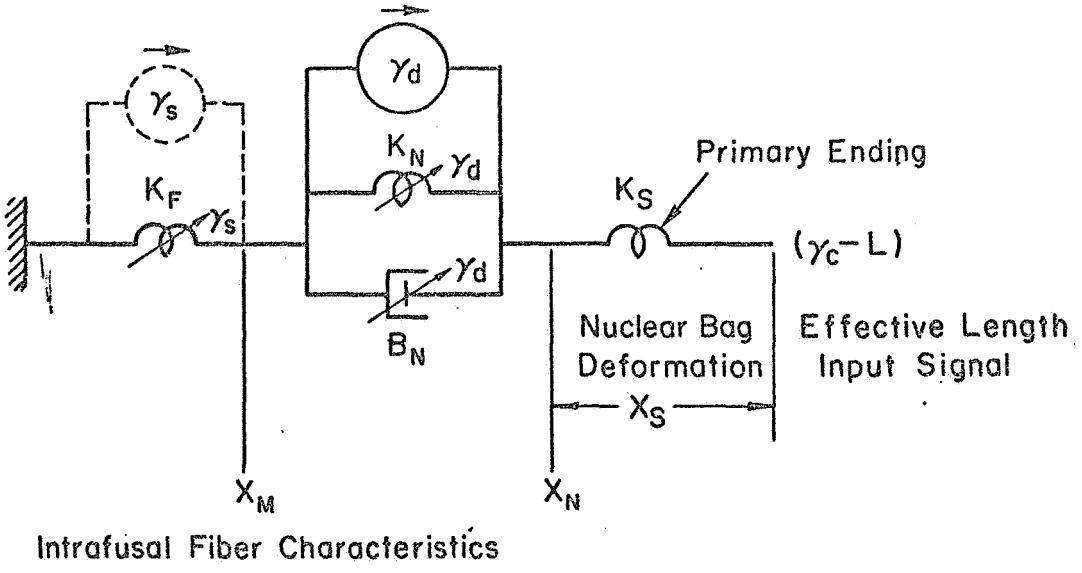

(b) Simplified Mechanical Network

Figure 15. Effective Spindle Characteristics

muscle in which the spindle is imbedded (Fig. 15). The nature of this monosynaptic coupling is such that increases in spindle firing frequency generate increases in the corresponding motorneuron firing frequency, and hence produce increasing motor unit contractile forces or resistance to stretch. The spindle axon also makes more complex connections which effectively inhibit the antagonist pool of motorneurons (Fig. 15). This reveals the underlying importance of the spindle/motorneuron feedback loop in stabilizing the length of the muscle. Influences tending, for example, to increase the length of the muscle, such as sudden increases in load, augment spindle activity which reflexively generates motor command signals tending to resist changes in length.

Of course the entire network of regulating mechanisms in the spinal cord is vastly more complex than the single mechanism we have presented, but in the development of our simplified model these more complicated aspects need not be included.

We now turn to the basic problem of actuating the feedback systems. Fundamentally, for the agonist to contract and the antagonist to relax, their alpha motorneurons must have firing rates which increase and decrease, respectively. This can be accomplished most directly by connections from higher centers to the alpha motorneurons. An alternative means to excite the alpha motorneurons is via the spindles by virtue of their contraction by gamma motorneuron excitation. Here, higher centers excite the gamma motorneuron, which contracts the intrafusal fiber, which leads to an increase in spindle discharge and thence to subsequent excitation of the alpha motorneuron and, finally, to muscular contraction. It appears that in some movements this is the route taken; in particular, in any steady voluntary effort the muscle tension and length may be determined by the rate of discharge from the gamma motor system. For example, the steady-state signals in gamma motorneurons which serve both agonist and antagonist muscles via their spindle systems may introduce tension preloads into the opposing muscles, which, as discussed previously, can exert profound changes on the neuromuscular actuation system time constants. In addition, such biases increase the spindle sensitivity by increasing the mean spindle discharge rate per unit deflection and by reducing any rectification effects caused as the spindle tends to become slack.

D. SIMPLIFIED NEUROMUSCULAR SYSTEM AND CLOSED-LOOP DYNAMICS

1. System Description

Although the microscopic details of the human operator's actuation system for even the simplest of motions are enormously complicated from a component standpoint, the actions of the overall system can still be modeled simply if component ensembles are used. The connections between these ensembles will depend greatly on the type of neuromuscular system motions involved. In this paper we are concerned primarily with neuromuscular system operations in which the command inputs are random and the motion outputs are exerted on spring-restrained low inertia manipulators.

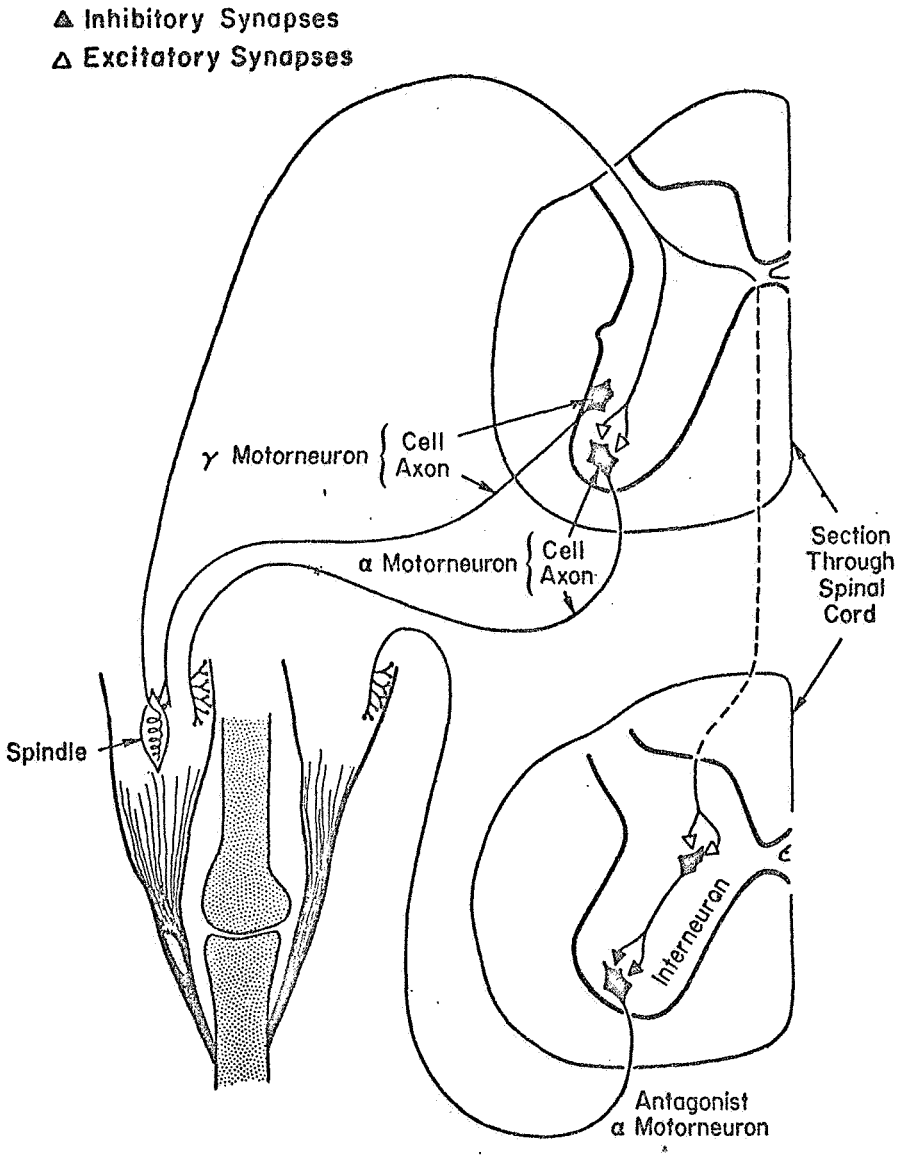

REFLEX ARCS OF MUSCLE SPINDLE

Fig 15

For this situation an appropriate neuromuscular system can be made up by connecting ensembles of the components described in the previous section into the equivalent system shown in Fig. 16. For other physical situations different neuromuscular system block diagrams will apply, e.g., see Refs. 3 and 12.

The block diagram of Fig. 16 shows perturbation operations about steady-state operating points. Consequently, all the signals indicated can be either positive or negative and the agonist/antagonist relationships are subsumed in the composite diagram (a block diagram of an agonist/antagonist operation with absolute level signals can be constructed by simply duplicating the Fig. 16 diagram, then connecting the two back to back with the limb rotation, θ, being a sum of the two outputs).

The spindle ensemble provides in one entity (1) the feedback of θ; (2) some series equalization, $K_{sp}(T_K s + 1)/(aT_K s + 1)$; (3) the source of one command to the system, γ_c; and (4) a means of spindle equalization and bias adjustment, γ_b. The spindle output differential firing rate, Δf_s, is summed with an alpha motorneuron command, α_c, with the result, after conduction and synaptic delays, being an incremental alpha motorneuron firing rate, Δf_α. This in turn operates the muscles and manipulators, giving rise to the limb rotation which is then sensed by the spindle ensemble.

The effective damping in the muscle and manipulator dynamics transfer function, G_M, is an operating point adjustment set by the <u>total</u> gamma bias, γ_o. The bias can derive from either the steady-state values γ_{b_o} and γ_{c_o}, or both, from which the γ_b and γ_c motorneuron signals represent perturbations. This dependence of muscle manipulator damping on steady-state gamma motorneuron activity is indicated in the block diagram by the γ_o input into the G_M block. Here we are presuming that the alpha motorneuron command is not involved.

2. Closed-Loop Dynamics — Effects of Average Tension

The closed-loop dynamic characteristics of the neuromuscular system for γ_c inputs are indicated in Fig. 17 for two levels of tension. For a given steady-state tension setting, the closed-loop roots are indicated on the conventional root locus and the closed-loop real loops on the Bode root locus (Ref. 21 and Appendix D of Ref. 22). In both diagrams the small pure time delay, τ_α, within the loop is neglected. These plots show that as gain is increased the low frequency muscle/manipulator root, $1/T_{M_1}$, approaches the lead zero, $1/T_K$, of the spindle, while the high frequency muscle root, $1/T_{M_2}$, and the spindle lag, $1/aT_K$, approach one another, rendezvous, and break into a second-order pair. For a particular loop gain, e.g., that shown by the zero-dB line on the amplitude ratio portion of Fig. 17, the closed-loop dynamics for a gamma command input have the form

$$\frac{\theta}{\gamma_c} \doteq \left(\frac{K_{dc}}{1 + K_{dc}}\right) \frac{(T_K s + 1)e^{-\tau_\gamma s}}{(T'_K s + 1)(T'_{M_2} s + 1)\left[(aT_K)' s + 1\right]} \tag{18}$$

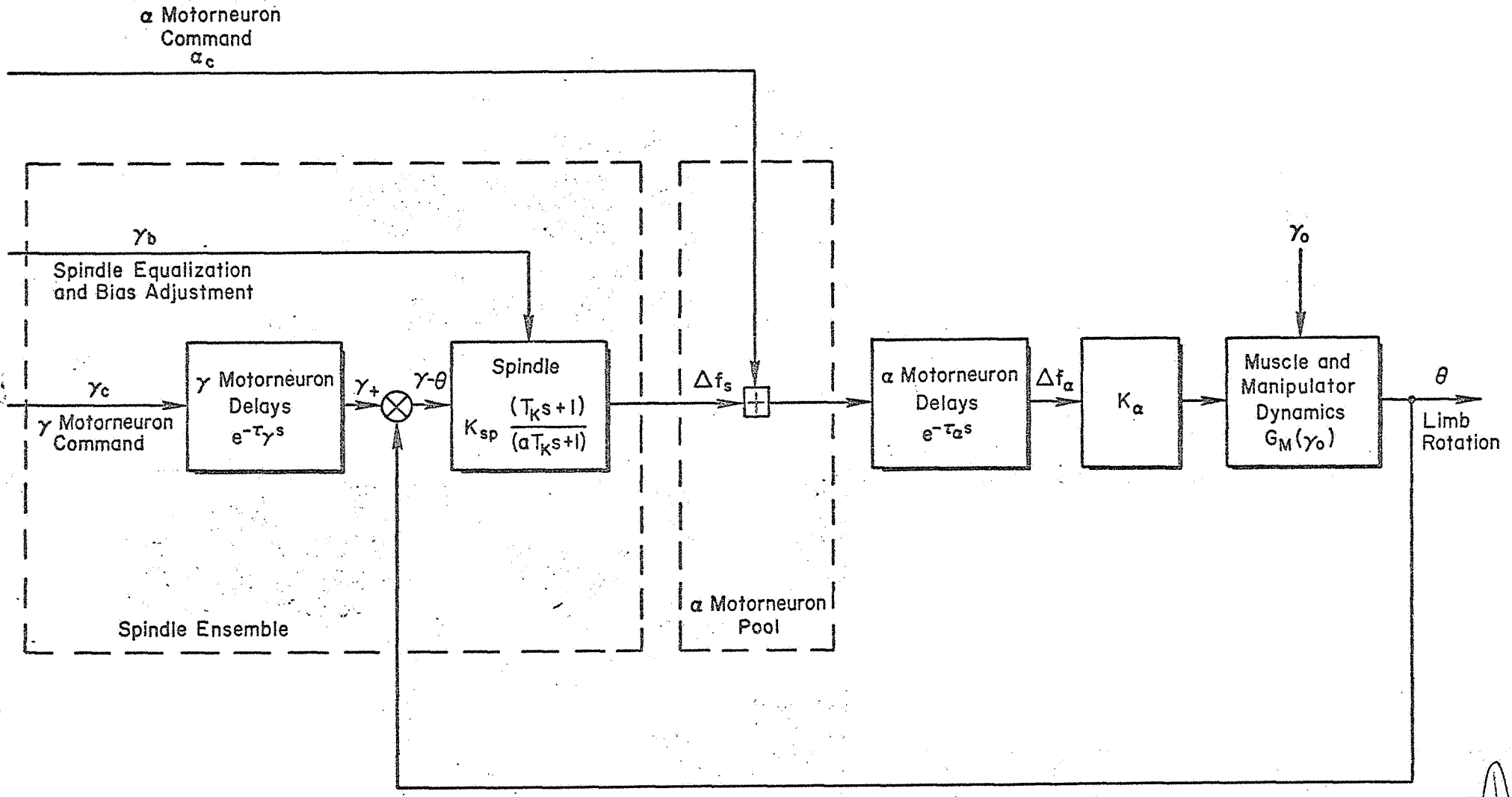

Figure 16. Elementary Neuromuscular System Model

Here K_{dc} is the dc gain of the open-loop system, τ_γ is the net delay in the gamma motorneuron pathways from the presumed point of command insertion in higher centers to the spindles, and the denominator time constants are primed to indicate that they are closed-loop quantities. Asymptotic plots of the open-loop $|\theta/(\gamma-\theta)|$ and closed-loop $|\theta/\gamma|$ are also given on the amplitude ratio plots of Fig. 17. On these the open-loop poles and zeros coincide with breakpoints of the solid-line asymptotes, whereas the closed-loop poles and zeros are indicated by breakpoints on the dashed or dotted asymptotes.

Consider now the effect of tension variation on the neuromuscular system dynamics indated in the plot. For a typical low tension condition (see the top amplitude ratio and related phase plot), defined by the steady-state tension, P_1, the muscle poles are located at $-1/T_{M1_{P_1}}$ and $-1/T_{M2_{P_1}}$. The closed-loop system will be given by

$$\left.\frac{\theta}{\gamma_c}\right]_1 \doteq \left(\frac{K_{dc}}{1+K_{dc}}\right)\frac{(T_K s+1)e^{-\tau_\gamma s}}{\left(T'_{K_{P_1}}s+1\right)\left(T'_{M2_{P_1}}s+1\right)\left[\left(aT_K\right)'_{P_1}s+1\right]} \tag{19}$$

or, in the mid-frequency range,

$$\left.\frac{\theta}{\gamma_c}\right]_1 \doteq \left(\frac{K_{dc}}{1+K_{dc}}\right)\left(\frac{T_K}{T'_{K_{P_1}}}\right)e^{-j(\alpha_1/\omega+\tau_{e1}\omega)} \tag{20}$$

This last expression corresponds to the phase description used in the approximate model described in Section B.

Presume now that the steady-state tension is changed by modifying γ_o; then the open-loop plot changes to the amplitude ratio and phase labeled "high tension." On these, the low and high frequency muscle factors are decreased to $1/T_{M1_{P2}}$ and increased to $1/T_{M2_{P2}}$, respectively (for simplicity, the spindle lead, $1/T_K$, and lag, $1/aT_K$, are assumed to be unmodified by the tension change). With the mid-frequency gain unchanged, the closed-loop dynamics are modified significantly. The low frequency lag/lead is more widely spaced, giving rise to a larger low frequency phase lag (i.e., $\alpha_2 > \alpha_1$) as seen in mid-frequencies; and the high frequency phase lag is substantially reduced (i.e., $\tau_{e2} < \tau_{e1}$). This demonstrates that the extremely simple neuromuscular system model described in Fig. 17 is qualitatively compatible with the data summarized in Section B and the physiological "component" characteristics of Section C. These results lend strong support to the neuromuscular system structure and connections presumed in Fig. 17. They also provide detailed functional roles within this system for the behavioral characteristics manifested by the muscle/manipulator and muscle spindle components when operated as separate entities.

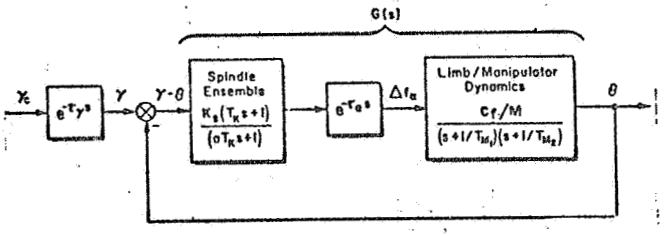

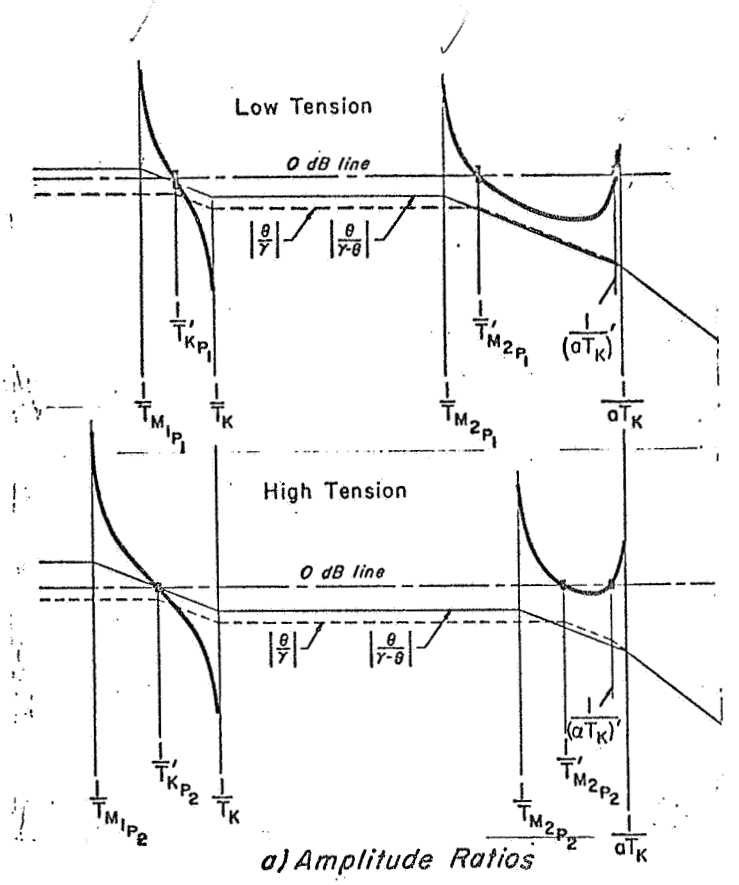

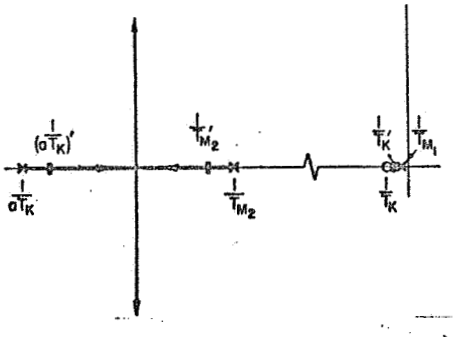

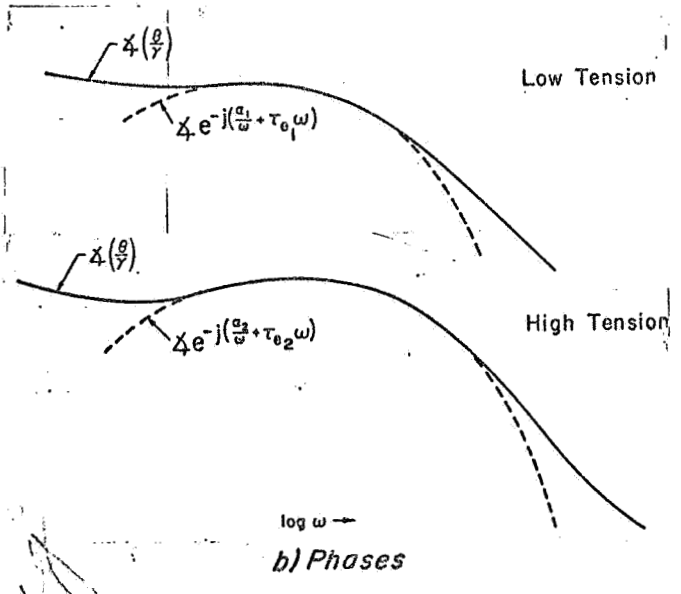

Figure 22. Root Loci of Neuromuscular Subsystem Dynamics with Two Levels of Tension

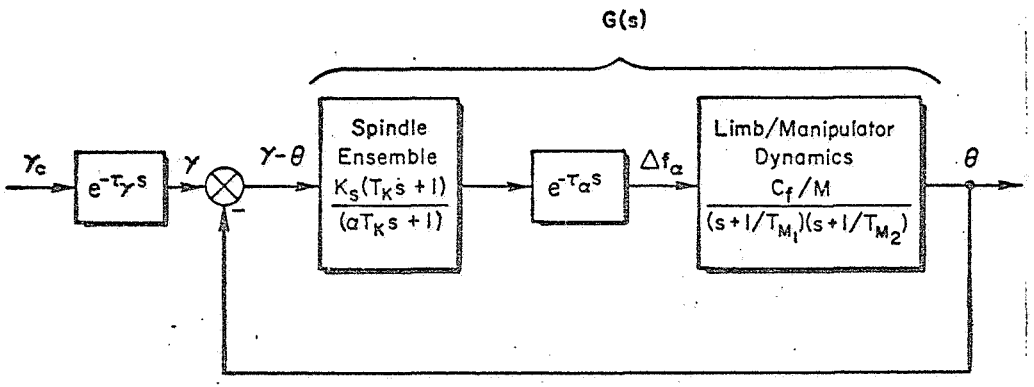

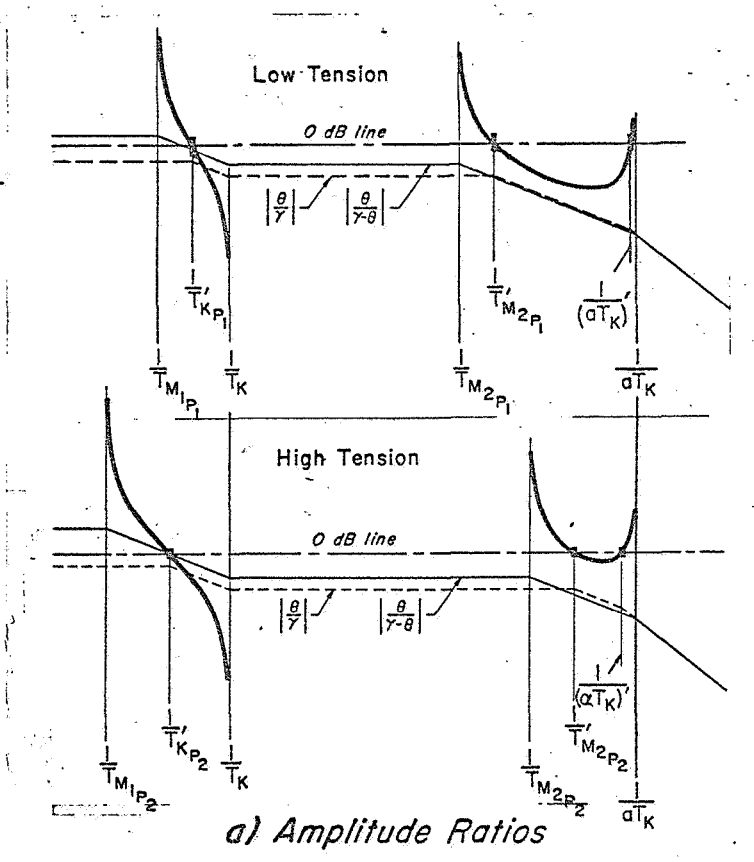

a) Amplitude Ratios

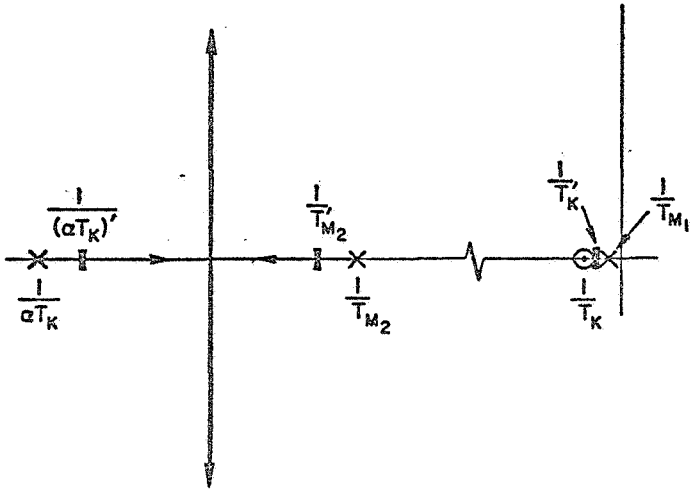

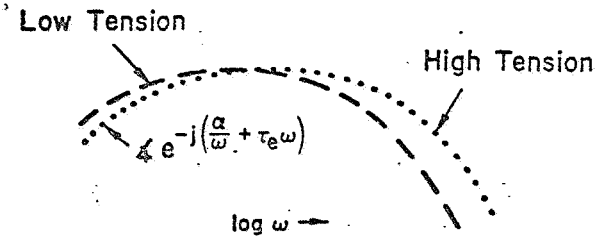

b) Approximate Phases

ROOT LOCI OF NEUROMUSCULAR SUBSYSTEM DYNAMICS WITH TWO LEVELS OF TENSION

While the behavior of the model closely approximates the original experimental data, it is essential to note some caveats. These are of two kinds — quantitative difficulties and oversimplified descriptions. For the first, suffice it to say that no data currently exist on spindle and muscle/manipulator ensembles for the motions for which the basic α and τ_e data are derived. Consequently, data on component ensembles cannot yet be shown to yield the closed-loop results already observed. Data of this nature for the muscle groups should be fairly simple to obtain, although those for the spindle ensembles are not presently within the possibility of direct experimental validation. If, however, the neuromuscular system structure presented here is assumed *a priori*, then *in situ* spindle implicit "measurements" can be obtained by suitable operations with the overall system and muscle subsystem data. The second point, that of oversimplification, is by no means as difficult to alleviate. For example, the muscle contains a series elastic component which makes the muscle/manipulator combination a third-order system. For spring-restrained low inertia manipulators this component is much larger than the other elements and thus has been neglected in this discussion. However, for other restraints it can be important; this is currently being investigated. In addition, we are working on alternative hookups of the neuromuscular system components.

SYMBOLS

a	Constant in Hill's equation; spindle lead/lag ratio
b	Constant in Hill's equation
B_c	Manipulator damping
$B_M(P_o)$	Equivalent damper for muscle system
B_N	Small signal equivalent damper (under γ_d control)
C_d	Constant of proportionality
C_f	Constant of proportionality
C_{f_s}	Constant of proportionality for primary ending firing rate
d_f	Fiber diameter
f	Average nerve firing rate in pulses/sec
f_o	Operating point average firing rate
f_{max}	Muscle firing rate producing tetanus
Δf_α	Incremental alpha motor neuron firing rate
F	Contractive force
$G_M(\gamma_o)$	Muscle and manipulator dynamics
i	Summation index
$j\omega$	Imaginary part of the complex variable, $s = \sigma \pm j\omega$
K_c	Controlled element gain; manipulator spring gradient
K_{dc}	The dc gain of the open-loop muscle-spindle system
K_F	Small signal equivalent spring (under γ_s control)
K_M	Equivalent spring gradient for muscle system
K_N	Small signal equivalent spring (under γ_d control)
K_p	Human pilot gain
K_S	Small signal equivalent spring for the nuclear bag region of a muscle spindle
K_{sp}	Spindle gain
K_α	Muscle sensitivity to alpha motorneuron firing
L	Actual length of muscle
L_o	Operating point length of muscle
ΔL	Length of muscle shortening
m	Integer
ms	Millisecond
M	Limb + manipulator inertia

P	Tension
P_o	Operating point tension
P_T	Tetanic tension
P_1, P_2	Particular operating point tensions
s	Complex variable, $s = \sigma + j\omega$; Laplace transform variable
T	Time constant
T_I	General lag time constant of human pilot describing function
T_K, T_K'	Lead and lag time constants in precision model of human pilot describing function
$\frac{1}{T_{K_{P_1}}'}, \frac{1}{T_{K_{P_2}}'}$	Closed-loop pole for tension P_1 or P_2
$\frac{1}{aT_K}$	Open-loop spindle model pole
$\frac{1}{(aT_K)'}$	Closed-loop spindle model pole
T_{lag_i} T_{lead_i}	General lag and lead time constants
T_L	General lead time constant of human pilot describing function
$\frac{1}{T_{M_1 P_1}}, \frac{1}{T_{M_1 P_2}}$	Low frequency muscle-manipulator root for tension P_1 or P_2
T_N	First-order lag time constant approximation of the neuromuscular system
T_{N_1}	First-order lag time constant of the neuromuscular system
V	Velocity of contraction
V_o	Operating point velocity
ΔV	Differential velocity of contraction
$Y_c(j\omega)$	Controlled element (machine and display) transfer function
Y_p	Pilot describing function
α	Low frequency phase approximation parameter
α_c	Alpha motorneuron command
α_1	Low frequency phase approximation parameter for tension P_1
α_2	Low frequency phase approximation parameter for tension P_2
γ	Gamma command following gamma motorneuron delay
γ_b	Gamma bias input due to γ_d
γ_{b_o}	Steady-state value of γ_b

γ_c	Gamma command input due to γ_s
γ_{c_o}	Steady-state value of γ_c
γ_d	Gamma input due to dynamic gamma motorneuron
γ_o	Total gamma bias
γ_s	Gamma input due to static gamma motorneuron
ζ_M	Damping ratio of limb/manipulator system
ζ_{M_o}	Minimum damping ratio of limb/manipulator system
ζ_N	Damping ratio of second-order component of the neuromuscular system
θ	Limb rotation
μm	Micrometer
σ	Real axis of complex plane
τ	Pure time delay
τ_e	Effective time delay
τ_{e_1}	Effective time delay for tension P_1
τ_{e_2}	Effective time delay for tension P_2
τ_α	Net time delay in the alpha motorneuron pathway
τ_γ	Net time delay in the gamma motorneuron pathways
$\Delta\varphi_{low}$	Incremental low frequency phase angle
ω	Angular frequency, rad/sec
ω_i	Forcing function bandwidth
ω_M	Undamped natural frequency of limb/manipulator system, $\sqrt{K/M}$
ω_N	Undamped natural frequency of second-order part of the neuromuscular system
$\doteq$	Approximately equal to
$\measuredangle$	Angle of
dB	Decibels; $10 \log_{10}$ ( ) if a power quantity, e.g., spectrum; $20 \log_{10}$ ( ) if an amplitude quantity, e.g., Y_p
$\lvert\ \rvert$	Magnitude
Σ	Summation
$\uparrow$	Increase
$\downarrow$	Decrease
∂	Partial derivative

REFERENCES

1. Elkind, J. I., and C. D. Forgie, "Characteristics of the Human Operator in Simple Manual Control Systems," IRE Trans. on Automatic Control, Vol. AC-4, May 1959, pp. 45-55.

2. McRuer, Duane, Dunstan Graham, Ezra Krendel, and William Reisener, Jr., Human Pilot Dynamics in Compensatory Systems: Theory, Models, and Experiments with Controlled Element and Forcing Function Variations, AFFDL TR-65-15, July 1965.

3. Young, Laurence R., and Lawrence Stark, Biological Control Systems—A Critical Review and Evaluation, Developments in Manual Control, NASA CR-190, Mar. 1965.

4. Jex, H. R., J. D. McDonnell, and A. V. Phatak, A "Critical" Tracking Task for Man-Machine Research Related to the Operator's Effective Delay Time. Part I: Theory and Experiments with a First-Order Divergent Controlled Element, NASA CR-616, Nov. 1966.

5. Okabe, Y., H. E. Rhodes, L. Stark, and P. A. Willis, Transient Responses of Human Motor Coordination System, MIT Res. Lab. Elec. Quar. Progress Rept. No. 66, July 1962, pp. 389-395.

6. Houk, James Charles, Jr., A Mathematical Model of the Stretch Reflex in Human Muscle Systems, Master of Science Thesis, MIT, 1963.

7. McRuer, Duane, "Remarks on Some Neuromuscular Subsystem Dynamics," IEEE Trans. on Human Factors in Electronics, Vol. HFE-7, No. 3, Sept. 1966.

8. Wilkie, D. R., "The Mechanical Properties of Muscle," Brit. Med. Bull., Vol. 12, No. 3, 1956, pp. 177-182.

9. Granit, Ragnar, "Neuromuscular Interaction in Postural Tone of the Cat's Isometric Soleus Muscle," J. Physiol., Vol. 143, 1958, pp. 387-402.

10. Crowe, A., and P. B. C. Matthews, "The Effects of Stimulation of Static and Dynamic Fusimotor Fibres on the Response to Stretching of the Primary Endings of Muscle Spindles," J. Physiol., Vol. 174, 1964, pp. 109-131.

11. Crowe, A., and P. B. C. Matthews, "Further Studies of Static and Dynamic Fusimotor Fibres," J. Physiol., Vol. 174, 1964, pp. 132-151.

12. Stark, L., Neurological Organization of the Control System for Movement, MIT Res. Lab. Elec. Quar. Progress Rept. No. 61, Apr. 15, 1961, pp. 234-238.

13. Wilkie, D. R., "The Relation Between Force and Velocity in Human Muscle," J. Physiol., Vol. 110, 1950, pp. 249-280.